Evaluation of CLC as a BECCS technology from tests on woody biomass in an auto-thermal 150-kW pilot unit

Øyvind LANGØRGEN [*], Inge SAANUM, Roger KHALIL, Nils Erland L. HAUGEN

SINTEF Energi AS (SINTEF Energy Research), Trondheim, Norway

ARTICLE INFO

ABSTRACT

In this work, woody biomass is converted by chemical looping combustion (CLC) in the auto-thermally operated 150-kW pilot unit at SINTEF Energy Research in Norway, using ilmenite as an oxygen carrier. The pilot unit consists of two inter-connected circulating fluidized bed reactors, being the air and fuel reactor, respectively. The unit is simplified compared to many other lab and pilot units by not having a carbon stripper. The aim of the present study is to evaluate the main performance parameters when operating a relatively large CLC unit in auto-thermal mode, using a cheap natural mineral, ilmenite, as oxygen carrier. Another aspect with the tests is to verify if the omission of a carbon stripper can provide high enough capture efficiencies for solid fuels as biomass, with a large share of volatiles and a char remnant with high reactivity. As a comparison, tests with petcoke were performed, to assess the effect when using a fuel with a low share of volatiles and slow char conversion. The results imply that CO_2 capture efficiencies can be well above 95 % in a larger industrial unit operating on biomass, even without a carbon stripper, but that a carbon stripper is definitely needed for fuels with less volatiles and low char reactivity.

1. Introduction

The IPCC is clearly stating that immediate and deep reductions of greenhouse gas emissions are needed to limit global warming to 1.5 °C (IPCC Working Group III report to Sixth Assessment Report 2022). Global GHG emissions must peak before 2025, net zero CO_2 emissions should be reached in 2050–2055, and from there, large net negative CO_2 emissions will be needed. Most emissions mitigation pathways that are likely to limit global warming to 1.5 - 2 °C by 2100, include CO_2 capture and storage (CCS) as one of several important measures. The Net-Zero Emissions scenario from IEA estimates a total CO_2 capture of 7.6 GtCO$_2$ per year by 2050 to be net zero (IEA 2021). Other scenarios show CO_2 capture by 2050 in the range 5.5 – 18.5 GtCO$_2$ per year (IPCC 2018). Even though there are large variations between different scenarios, a huge CCS deployment is in any case foreseen.

Importantly, a large share of the needed CCS capacity will be allocated to carbon dioxide removal (CDR) technologies. The two main approaches to CDR are bioenergy with carbon capture and storage (BECCS) and direct air carbon capture and storage (DACCS), where BECCS plays the dominant role. The scenarios likely to limit warming to 2 °C, estimate annual BECCS capacity in 2050 in the range of 0.52 – 9.45

GtCO$_2$/year, with a median value of 2.75 GtCO$_2$/year (IPCC Working Group III report to Sixth Assessment Report 2022). This is equivalent to 2750 BECCS plants, each capturing and storing one million tonnes of biogenic CO_2 per year. This involve several challenges, not at least how to assure that the huge amounts of biogenic feedstocks can be supplied sustainably.

Chemical Looping Combustion (CLC) is a well-suited technology for BECCS that can provide negative CO_2 emissions at high efficiency and low cost (Rydén et al., 2017). CLC can be described as a type of an oxy-fuel combustion process, however, without the need for a cryogenic air separation unit to produce oxygen for combustion. Instead, air separation is an inherent part of the process, where a solid metal oxide material (MeO) is being oxidised by taking up oxygen from the air in an air reactor, and reduced by releasing the oxygen in the fuel reactor, where it is used to combust the fuel. The metal oxide material is therefore often called the oxygen carrier (OC) material. The very basic principle of CLC is shown in Fig. 1. The air and fuel are not mixed and the exhaust gas from the fuel reactor is thereby not diluted with nitrogen from the air. It will ideally contain only CO_2 and H_2O, and the CO_2 can easily be separated just by condensation of the H_2O. The two reactors are most commonly being designed as fluidised bed (FB) reactors, and the
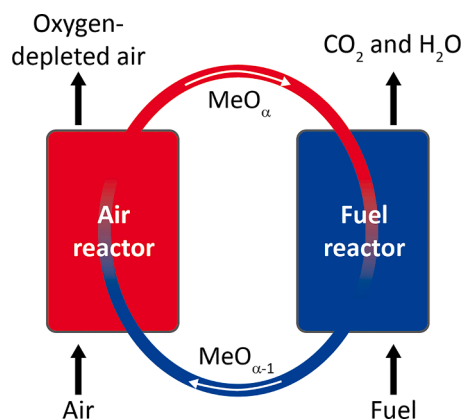

Fig. 1. Basic principle of Chemical Looping Combustion (CLC).

OC material will be in the form of small particles that will act as the bed material of the FB reactors. The OC material is a cornerstone of the CLC process. Much work has been conducted on their development, as it is critical to have materials with high oxygen transport capacity and long lifetime. In addition, the OC should be environmentally viable and preferably have low production cost. The OC materials have mainly been based on oxides of Fe, Mn, Cu, Ni and Co, either synthetically made, or cheaper alternatives from natural ores. An example of such natural ores is ilmenite, which has been widely used within CLC research and development.

In the real process there are two important issues that can make the CLC process deviate from the ideal situation shown in Fig. 1. Firstly, the oxygen provided with the OC material may not be enough to fully convert the fuel. A small quantity of unconverted gases and particulates may leave with the fuel reactor flue gas. From an efficiency and cost perspective, fuel conversion must be close to 100 %. To achieve this, a small stream of oxygen injection just downstream of the fuel reactor is needed to fully combust any unconverted compounds. The oxygen for this so-called oxygen-polishing step is one of the most important parameters to evaluate in CLC, since it must be provided from an external source and represents a cost and efficiency loss. Secondly, char particles that are not fully converted in the fuel reactor may follow the reduced OC material back to the air reactor. There they will burn immediately in the hot, oxygen-rich atmosphere, and the generated CO_2 will leave with the air reactor outlet gas. Since it is only the CO_2 from the fuel reactor that is captured in the CLC process, any CO_2 from the air reactor represents a loss in capture efficiency.

Because of the above, a carbon stripper between the fuel and the air reactor has generally been considered needed in CLC of solid fuels to achieve capture efficiencies close to 100 % (Sun et al., 2015). The use of a carbon stripper is most important for solid fuels with low-reactivity char since they require long residence time for complete gasification (Sun et al., 2015). A carbon stripper separates the char particles from the reduced OC particles coming from the fuel reactor. This is typically done by utilizing the difference in terminal velocity of the low-density char particles compared to the high-density OC particles. The separated char particles are transported back to the fuel reactor; hence, reducing loss of carbon to the air reactor. Several carbon stripper designs exist (Gong et al., 2021), but they all increase the complexity of the CLC unit, as well as operational costs.

CLC has shown potential for high thermal efficiencies and high CO_2 capture efficiencies. Net electric efficiency penalties of only 2.5 and 4 %-points compared to relevant reference technologies without CO_2 capture has been reported with coal as fuel (Spinelli et al., 2016; Lyngfelt and Leckner, 2015). Net electric efficiency penalty is also shown to be lower than other comparable technologies with CO_2 capture, with 5 %-points gain compared to an oxyfuel circulating fluidized bed (CFB) case (Spinelli et al., 2016), and 6.5 %-points gain compared to

a CFB with amine (MEA) absorption (Fu et al., 2021), the latter study using petcoke as fuel. At the same time, both studies showed much higher CO_2 capture efficiency for the CLC cases than the reference capture technologies, 95.5 % vs 91.5 % and 97.5 % vs 90.0 %, respectively. The potentially low energy penalty and the high capture efficiency is beneficial to the economy of the CLC process. A CO_2 avoidance cost of less than 26 €/tonne has been estimated in an earlier study (Lyngfelt and Leckner, 2015), using coal as fuel and a standard large CFB boiler for power production as reference technology. An avoidance cost in the range 18.6 – 33 €/tonne have been found in a recent public study (Roussanaly et al., 2022) from the European-Chinese CHEERS project, using a CFB without capture as the reference plant, and petcoke as fuel. In comparison, the same study finds the avoidance cost of CFB with MEA capture to be in the range 64.5 - 71.5 €/tonne.

The CLC process has, during the last two decades, been operated in nearly 50 smaller CLC lab and pilot units in the range 0.3 kW_{th} to 1 MW_{th} for a total of more than 11 000 h using different fuels, both gaseous and solid, and different oxygen carrier materials (Lyngfelt et al., 2019). During the last 15 years, significant developments have been made, especially in CLC of solid fuels, and about 20 lab- and pilot units have reported results (Adánez et al., 2018). More recently, a demo unit is under construction in China as part of the European-Chinese cooperating project "CHEERS" (Yazdanpanah et al., 2018), with a nominal capacity of 3 MW_{th} and maximum capacity of 4 MW_{th}.

CLC using biomass (Bio-CLC) has been studied less than CLC with coal, but an increasing number of studies are now available as BECCS has gained more interest globally. Bio-CLC can draw on experience from conventional fluidized bed combustion technology for biomass, which is commercially available at large scale and has been utilized for many years (Grammelis et al., 2011). Nanjing University operated a 10 kW_{th} CLC pilot plant with sawdust (Shen et al., 2009), while CSIC investigated CLC of forest and agricultural residues in a 0.5 kW_{th} unit (Mendiara et al., 2018; Pérez-Astray et al., 2019). Chalmers University has performed tests in both a 10 kW_{th} and a 100 kW_{th} pilot unit with different biomass fuels, such as biochar and crushed wood pellets (Schmitz and Linderholm, 2018), using a manganese ore as oxygen carrier, yielding fuel conversion beyond 90 % and carbon capture efficiencies above 95 %. TU Darmstadt has operated their 1 MW_{th} pilot plant with mixtures of coal and torrefied biomass (Ohlemüller et al., 2017). The Technical University of Vienna did experiments with wood and bark pellets using a synthetic C28 oxygen carrier in their 80 kW pilot, achieving very high fuel conversion (Fleiß et al., 2023). CLC of biomass was performed by Chalmers, VTT, and SINTEF, using CLC pilot units of up to 150 kW_{th} size, plus a larger semi-commercial CFB unit of up to 4 MW_{th} biomass feed (Rydén et al., 2017). SINTEF Energy Research has demonstrated CLC operation with biomass pellets using ilmenite as oxygen carrier (Langørgen and Saanum, 2018; Langørgen et al., 2022). A general conclusion from all the above experimental work is that CLC with biomass is a feasible technology that can achieve high fuel conversion and CO_2 capture efficiency, thus being a relevant technology option for BECCS.

The tests reported in this study are performed in the 150 kW_{th} CLC pilot unit at SINTEF Energy Research in Norway, using biomass as fuel and ilmenite as oxygen carrier (OC) material. Biomass fuel feed rates are in the range 101–129 kW. The main objectives are to investigate process performance in terms of fuel conversion, oxygen demand, and capture efficiency, and to verify that auto-thermal operation can be achieved. The unit does not contain a carbon stripper, and it is of interest to see if this simplified design can provide high enough CO_2 capture efficiencies when operating with woody biomass. Due to its large share of volatile content, more than 70 %, and a char remnant that has high reactivity, woody biomass is considered being a reactive fuel. For comparison, the performance and capture efficiency are also evaluated for less reactive fuels, by mixing in some petcoke together with the biomass.

2. Experimental

2.1. Reactor system and design

The reactor system of the 150 kW CLC pilot unit that is used for this study consists of two interconnected circulating fluidized bed (CFB) reactors, as shown in Fig. 2. Both the air reactor (AR) and the fuel reactor (FR) are 6 m tall of which the first 1 m is a conical bottom section. The remaining 5 m cylindrical sections have internal diameters of 230 mm (AR) and 154 mm (FR). The reactors are designed to operate in fast fluidization mode, which is the normal mode for a conventional CFB plant. The reactor superficial gas velocity is in the range 3 – 5 m/s. The smaller FR diameter is chosen to give the wanted fluidization mode with a low amount of steam injection. The overall OC circulation rate is mainly controlled by the fluidization of the AR, i.e., the amount of air fed to the process.

The metal oxide particles circulate between the reactors via the cyclones and the loop-seals, which prevent gas mixing between the reactors. In addition, particles are also transferred from the fuel reactor to the air reactor through the lifter, which extracts particles from the bottom of the fuel reactor. The lifter is generally required to achieve the targeted overall OC circulation rate. In addition, it gives higher degree of operational flexibility. As an example, it allows the fluidization mode of the FR to be reduced from fast to turbulent mode, since particles can be returned to the AR via the lifter. The lifter share of the overall OC circulation rate is controlled by the balance between fluidizing gas injected in the lifter bottom and fluidizing gas to the FR. The OC transport through the lifter is actually very sensitive to the amount of lifter fluidization gas and rather small variations can shift the OC inventory between the reactors. Having control of the lifter fluidization makes it a very useful tool for control of the solid circulation. The total reactor system height from bottom of the lifter to the top of the cyclones is 7 m.

The loop-seals were originally of the divided type, where a share of

the OC flow could be directed back to the reactor from which it came. However, the divided loop-seals made it more difficult to control the pressure balance and OC circulation of the system. The internal legs were therefore blocked, and the loop-seals are now of single-direction type as shown in Fig. 2. The FR can be fluidized with nitrogen or steam. Since the diameter of the FR is less than for the AR, only a small amount of gas is normally needed in addition to the flue gas being generated by conversion of the solid fuel, at least for reactive fuels like biomass. The bottom lifter is fluidized only with nitrogen. Then the flow can be controlled with a mass flow controller that has high accuracy at the small flows required. It should be noted that nitrogen for fluidization is relevant only at lab or pilot scale. For an industrial plant, recycled flue gas will be used for fluidization, except for the AR fluidization.

The only electrical heating used during CLC operation, is a 30-kW pre-heater for the primary air to the AR. This means that the system is temperature-wise working rather equal to what must be the case for a large-scale CLC unit, i.e., it operates in auto-thermal mode. Auto-thermal operation of a reactor system at this relatively small scale is challenging because of the high relative heat loss due to the large surface to volume ratio. The reactors are made of high-temperature steel, MA253, and does not have internal refractory lining. To limit heat losses, the reactor system is made very compact, as can be seen in the CAD drawing shown in Fig. 3. The reactors, downcomers and loop-seals are placed close to each other, making it possible to wrap the main parts into one common insulation, in addition to the use of separate insulation on each reactor. Auto-thermal operation also puts more constraints on the reactor temperatures and oxygen carrier circulation. The possible operating range is smaller since it cannot be chosen just from pressure balance, fluidization mode, or FR specific inventory.

The system was originally designed for operation with methane as fuel gas at a maximum fuel power of 150 kW$_{th}$ (Bischi et al., 2011; Langørgen et al., 2017) and has later been modified to solid fuel feeding (Langørgen and Saanum, 2018). The solid fuel feeding system consists of
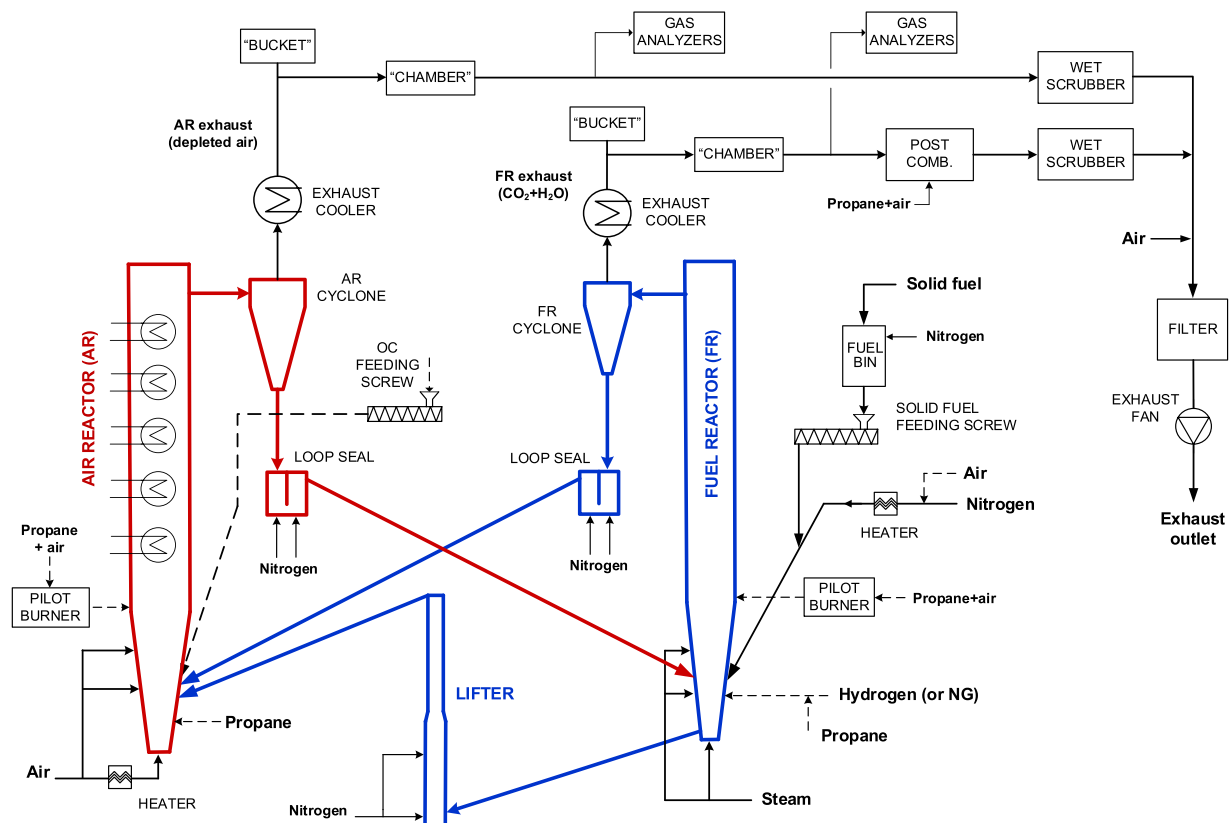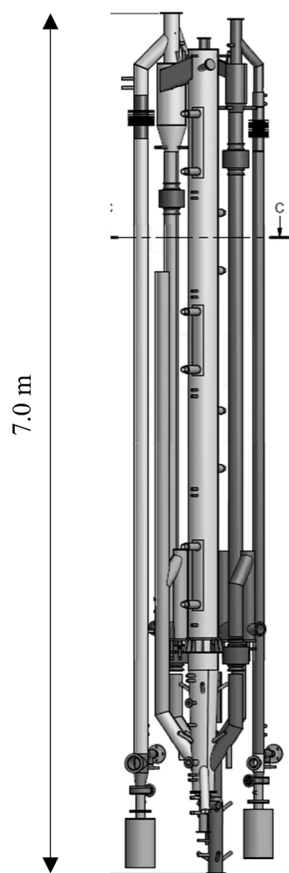

Fig. 2. Simplified process flow diagram of the whole 150 kW$_{th}$ CLC pilot unit.

Fig. 3. CAD model of the main reactor system. AR in mid position in front. AR cyclone, downcomer, loop-seal, and pipe-in-pipe exhaust cooler (from top outlet cyclone and downwards) on left side. The same for FR on right side. FR reactor behind (not seen).

a double-valve lock-hopper fuel bin that can be filled during operation, a solid fuel feeding screw that controls the amount of solid fuel being fed, and a fuel injection pipe where the fuel particles falling from the screw are injected into the bottom part of the FR with nitrogen as the fuel carrying gas. A small positive flow of inert gas is fed from the fuel bin and through the whole feeding system using a mass flow controller. This will counteract varying pressure in the FR and secure against backflash of combustible gases. Two different volumetric feeding screws can be used. One larger and rugged feeding screw with a screw diameter of ⌀95 mm that is used for pelletized fuels. The rotational speed vs fuel feed rate is obtained from separate calibration measurements done before the CLC tests. For smaller fuel sizes, such as milled and pulverized fuels, a smaller and more accurate feeding screw with diameter ⌀60 mm and fine pitch is used. This volumetric feed screw has a more advanced system for calibration as well as a fuel bin just before the screw with a bottom agitator, ensuring an even flow down into the screw itself. There is also a feeding screw for oxygen carrier particles, with a double-valve lock hopper for OC feeding during operation. The OC particles are fed into the AR and a positive flow of air through the OC feeding system is used to adjust it to the fluctuating AR pressure, as well as to smooth the particle transport.

Both reactors are equipped with 30-kW electric air heaters plus fuel gas lances that are used during the heat-up sequence. For the FR, the fuel lance is used to provide hydrogen to the reactor. The advantage with hydrogen is its high reactivity, making the combustion zone stay down in the bed, close to the fuel injection lance. In the AR, only propane is available. The electric pre-heating of air to the FR through the fuel injection pipe is shut down well before injection of solid fuel is started. This is done to avoid the pipe being too warm for the fuel. If not, experience shows that the risk of fuel plugging is considerably increased.

When appropriate temperature levels are reached, injection of solid fuel commences, while air to the FR through the fuel inlet pipe is gradually decreased to zero and substituted with a smaller flow of nitrogen acting as the fuel carrying gas. At this point, full CLC operation is reached.

Each reactor has six pressure transmitters mounted along the reactor height, with most of them in the bottom part. There are also pressure transmitters in the bottom and top of the lifter, out of the cyclones, in the loop-seals as well as in the main air and steam supply lines. Continuous flushing of the pressure transmitters is employed to avoid plugging, using nitrogen for FR and air for AR transmitters. The small flow of flushing gas is controlled purely by small nozzles being at sonic condition. In addition, if plugging has occurred, the pressure transmitters can be individually pulsed with the same gases as for the flushing, using magnetic valves that are controlled from the operator screen. There are five temperature transmitters in each reactor, plus temperature measurements in the lifter, in the exhaust system and in each of the pre-heated inlet streams and in the fluidization steam line to the FR.

As shown in Fig. 2, the pilot unit also includes pipe-in-pipe exhaust gas coolers, particle separation "buckets" placed in a high-velocity 90-degree turn in the exhaust pipes, low velocity particle settling "chambers", suction pipes for gas composition measurements, a post-combustion chamber with a propane-fired pilot burner to ensure burn-out of remaining combustible components from the FR, wet scrubbers with fine water sprays to cool and clean the flue gas from particulates, a common bag filter unit for both FR and AR including exhaust fan, and an air inlet just upstream the filter unit to further dilute and cool the gas. The exhaust gas coolers were originally operated only using air as cooling medium. However, the cooling capacity was on the limit, so the cooling air is now wetted with fine water sprays, considerably increasing the cooling capacity. The particle separation "buckets" separate out the larger particles coming from the cyclones, this is especially useful during heat-up or process upsets when cyclone separation is not as stable and efficient as under normal operation. The settling "chambers" separate very small particles and fines, and is used as a simple way to reduce the loading on the equipment further downstream, including the gas analysis filters. Both the "buckets" and the "chambers" have a double-valve outlet section so they can be emptied during operation.

All flows of fuel gases, air and dry gases are controlled by mass flow controllers, whereas steam flows are controlled by steam valves. The rotational speed of the solid feeding screws and the exhaust fan is controlled by frequency converters. The process control system is based on a controller programmed using LabView. Operator screens and PC is placed in a separate control room. The control system is operated in manual mode, meaning that all valves, screws and exhaust fan speeds, pre-heat temperatures, burner controls, etc., are manually set by the operator from the control screen. No automated control loops have been included so far.

There is also a separate emergency shut-down system (ESD) that will shut down all fuel and gas flows by normally closed valves, and open for a small nitrogen fluidization of the system by normally open valves. The ESD is triggered by reactors over-pressure, reactors over-temperature, two gas detectors measuring combustible gas around the reactor, too high temperature before bag filter unit, black-out of power supply, and emergency shut-down buttons placed around the pilot unit.

The composition of the outlet exhaust gas streams from the cyclones are monitored with on-line gas analyzers. The CO_2, CO and O_2 concentrations of the fuel reactor exhaust is measured with an Emerson Rosemount X-stream IR analyser. A Varian CP4900 Micro-GC is also connected to the fuel reactor exhaust. It measures gases such as H_2, CH_4, N_2, C_2 hydrocarbons and helium. Helium is fed to the fuel reactor as a trace gas and its concentration in the exhaust is used for mass balance evaluation. The Micro-GC also measures CO_2 and CO and therefore serves as a check of the IR analyser. The air reactor gas outlet is monitored with a Horiba PG-250 IR analyser, measuring CO_2, CO and O_2 concentrations. For the more recent tests, a second Micro-GC has been connected to the AR exhaust, to measure helium to see whether there is

some gas leakage between the reactors and to control and verify the CO_2 measurements of the Horiba analyser, being important for the capture efficiency calculation.

2.2. Fuels

The reference fuel is biomass pellets from Arbaflame. This is a steam-exploded wood pellet, giving a brown colour and a more water-repellent and less sticky biomass than standard white wood. The pellets have a diameter of 8 mm and typical length of 15 – 35 mm. Some quantity of the pellets is also milled and sieved to test smaller fuel sizes (cf. Fig. 4).

Table 1 shows composition and combustion data for the fuels tested. Two different compositions of the biomass pellets are given since two different batches (Arba1 and Arba2) are used. The Arba2 batch is of second-rate quality, and it contains more moisture than Arba1. Included in the table is also the Φ_0 value, the molar amount of O_2 needed for full conversion of the fuel per mole of carbon in the fuel, which is used in calculation of oxygen demand.

To test the CO_2 capture efficiency and fuel conversion when the fuel is less reactive, an increasing amount of petcoke is blended into the milled biomass fuel. The petcoke used is a low-sulfur Chinese petcoke that is dried, milled, and sieved into three different size fractions. Fig. 5 shows the petcoke in size fraction 315–500 μm. The petcoke is rich in carbon and have a very high heating value compared to many other solid fuels. The final delivered petcoke was nearly dry, with a moisture content of less than 1.0 wt-%. The feeding of petcoke particles may be associated with problems since the particles tend to be sticky when heated. This was experienced several times during the tests as the particles got stuck in the fuel injection pipe close to the reactor wall. However, by shutting down the pre-heater in the air/nitrogen line to the FR well before starting petcoke injection, as well as supplying enough room-temperature nitrogen as fuel carrying gas, the problem is avoided.

The fuel sizes for the biomass in Table 1 represents the three different variants shown in Fig. 4. First, whole pellets with diameter 8 mm and typical length about 30 mm, thereafter milled pellets that are sieved to sizes larger than 800 μm, and finally a milled and un-sieved variant with all the fines from the milling included, and where the smallest size is estimated to be about 0.01 mm. The petcoke is also tested in three variants. A larger size of 315–500 μm (cf. Fig. 5) and a smaller size of 100–315 μm. In addition, as for the biomass, a fraction containing the fines from the milling is tested. This is made from the 100–315 μm fraction mixed with 40 % of fines from the milling (< 100 μm).

2.3. Ilmenite oxygen carrier

Most of the tests in the pilot unit have been performed with ilmenite as oxygen carrier. The ilmenite has been provided by Titania AS, which operates an open-cast ilmenite mine in south-western Norway. The standard ilmenite from Titania has a relatively large size range of 10 – 350 μm. The 150 kW unit is designed for smaller particles than most other CLC lab and pilot units. The reason for this design choice is that it makes the unit able to use OC particles in the same size range as most

Table 1

Fuel composition (wt-%), oxygen requirement Φ0, and lower heating value (LHV). Values based on fuel as received (a.r.).

Fuel		Biomass pellets		Petcoke [**]
Batch		Arba1	Arba2	
C	wt-% a.r.	50.7	49.8	90.7
H	wt-% a.r.	5.8	5.4	3.9
O	wt-% a.r.	38.1	35.9	1.4
N	wt-% a.r.	0.01	0.1	1.7
S	wt-% a.r.	0.001	0.01	0.83
Ash (550 °C)	wt-% a.r.	0.48	0.31	(~ 0.2)
Fixed C	wt-% a.r.	19.4	18.0	(~ 90)
Volatiles	wt-% a.r.	75.2	73.2	(~ 8)
Moisture	wt-% a.r.	4.9	8.5	< 1.0
LHV	MJ/kg	19.29	18.69	30.0
Φ_0 [*]	mol/mol	1.06	1.05	1.13
Fuel size		8 × 30 mm	8 × 30 mm	315–500 μm
		0.8 - 3 mm		100–315 μm
		0.01 - 3 mm	0.01 - 3 mm	10 - 315 μm

(*) The molar amount of O2 needed for full conversion of the fuel per mole of carbon in the fuel.

(**) The ash, fixed carbon, and volatiles of the used batch of petcoke is not available. The data provided in parenthesis is from another batch from the same supplier and will be close to the actual petcoke used. The large difference compared to biomass is evident.

Fig. 5. Petcoke in size-fraction 315 – 500 μm.

commercially available catalyst materials. An additional benefit of using such small particles is that it results in an increased surface to volume ratio, and also possible reduced risk of fractures due to mechanical stresses. For most of the experiments, the ilmenite is therefore sieved to a range of 40 – 140 μm before being used in the pilot unit.

Some instabilities in the AR cyclone and downcomer were experienced during the tests. This was most likely caused by bridging and

Fig. 4. Wood pellets. 8 mm pellets; milled and sieved; milled and un-sieved (left to right).

particle build-up in the bottom of the cyclone, especially when operating at the highest temperatures. It has been questioned whether the use of so small OC particles could be one of the reasons for this problem. Two larger size fractions are therefore tested as well; 150 – 350 μm (cf. Fig. 6) and 50 – 250 μm, and this is found to improve the situation. The particle size distributions of the three ilmenite size fractions are shown in Fig. 7.

With the largest size fraction, the riser velocity is increased to compensate for the higher terminal velocity of the particles, and thus maintain the particle circulation. The compressor and air lines can manage this higher flow. However, since this pilot unit is not designed for such large particles, it results in a larger amount of excess air than optimal, reducing the overall process efficiency. The intermediate size fraction of 50 – 250 μm is shown to be a good alternative and is still within the design limits of the unit, achieving high enough circulation without too much air feed.

2.4. Performance parameters

2.4.1. Oxygen demand and gas conversion efficiency

The gases leaving the fuel reactor will normally not be fully converted, resulting in the need for an "oxygen polishing" step just downstream of the fuel reactor. In the oxygen polishing step, pure oxygen is fed to the hot exhaust stream to completely burn out remaining unconverted fuel components. The amount of oxygen needed for the polishing step is commonly considered to be equal to the so-called fuel reactor gas oxygen demand Ω_{OD}. It represents the ratio of the additional oxygen needed to completely convert the unconverted gases leaving the FR, to the stoichiometric amount of oxygen needed to fully convert all the combustible gases released in the FR. In our case, the FR gas oxygen demand is calculated as

$$\Omega_{OD} = \frac{0.5x_{CO,FR} + 2x_{CH_4,FR} + 0.5x_{H_2,FR} + 3x_{C_2H_y,FR}}{\Phi_0\left(x_{CO_2,FR} + x_{CO,FR} + x_{CH_4,FR} + 2x_{C_2H_y,FR}\right)}, \quad (1)$$

where Φ_0 represents the molar amount of O_2 needed for full conversion of the fuel per mole of carbon in the fuel, and x_i is the measured molar fraction of the ith species in dry gas. The parenthesis in the denominator gives the total molar amount of carbon in the FR outlet gases. The Micro-GC measures the sum of some C_2 molecules. It is here assumed they are C_2H_4 on average. This way of calculating the oxygen demand is convenient since it is calculated only from the gas analysis of the FR exhaust. However, in solid fuel CLC, there might be some losses of unconverted

Fig. 6. Sample of ilmenite 150 – 350 μm.

solid fuel particles out from the FR, mainly carbon-rich char. To reduce fuel losses and increase the CO_2 capture efficiency of the system, these particles should also be converted in the oxygen polishing step. The above oxygen demand calculation does not include this potential fuel loss, which will increase the actual oxygen demand.

From the FR oxygen demand calculation, the FR gas conversion efficiency can be defined as

$$\eta_{gas} = 1 - \Omega_{OD}. \quad (2)$$

This represents the efficiency of the oxidation of the fuel gases being released by devolatilization and gasification from the solid fuel in the FR. It should be as high as possible, ideally 100 %, meaning that all fuel gases released are oxidised fully to CO_2 and H_2O. However, even if it reaches 100 %, the actual fuel conversion in the FR might still be less than 100 % since some fuel could leave the FR as particulates (char).

2.4.2. CO_2 capture efficiency

In addition to possible char particles leaving together with the FR exhaust, there may also be a loss of char particles from the FR to the AR, following the oxygen carrier particle stream. This so-called "carbon slip" will immediately be oxidized to CO_2 in the high temperature and oxygen-rich atmosphere in the AR, before the CO_2 leaves the system with the AR exhaust. Since it is only the CO_2 that leaves the FR that will be captured and made available for permanent storage, the CO_2 out from the AR will cause the overall CO_2 capture efficiency to be lower than 100 %. The CO_2 capture efficiency is calculated as

$$\eta_{CO2\ capture} = \frac{carbon\ in\ fuel\ feed\ to\ FR\ -\ carbon\ out\ from\ AR}{carbon\ in\ fuel\ feed\ to\ FR}. \quad (3)$$

The carbon in the fuel feed is calculated from the carbon content of the fuel and the fuel feeding rate given by the screw feeder, which has been calibrated for the actual fuel. The carbon out from the AR is calculated from the total molar flow out from the AR and the measured CO_2 concentration. The total molar flow out from the AR is calculated from the total molar flow of N_2 out of the AR, being equal to N_2 fed to the AR with air and fluidization gases, and the concentrations of O_2 and CO_2 at the outlet, since they will be the only gases in addition to N_2. The capture efficiency calculated this way considers CO_2 out from the AR as the only carbon not being captured, and requires that all unburnt fuel components out from the FR is converted to CO_2 in the oxygen polishing step and captured.

The 150 kW pilot unit at SINTEF Energy Research, originally designed for gaseous fuels, does not have a carbon stripper and some char will therefore be lost from the FR to the AR, especially through the bottom lifter. CLC systems for solid fuels will normally be equipped with a carbon stripper to convert most of these char particles before they reach the AR, thereby increasing the capture efficiency of the system. Especially for slowly reacting fuels, such as petcoke, this is important. However, from earlier and present tests in the 150 kW pilot unit at SINTEF Energy Research, it is shown that high capture efficiencies can be achieved for a reactive fuel as biomass, even without a carbon stripper.

2.4.3. Oxygen carrier circulation and inventory

There is no direct way of measuring the oxygen carrier circulation rate between the reactors in the pilot unit. One way to estimate it, is to use the reactor pressure recordings in the AR riser. A theoretical riser mass flow can be estimated by the pressure difference (Δp) between the two upper pressure transmitters, the difference in height between the transmitters (Δh), the superficial gas velocity (u_0), the terminal velocity of the OC particles (u_t), the reactor riser flow area (A), and gravitational acceleration (g):

$$\dot{m}_{riser} = \frac{A}{g}\frac{\Delta p}{\Delta h}(u_0 - u_t). \quad (4)$$
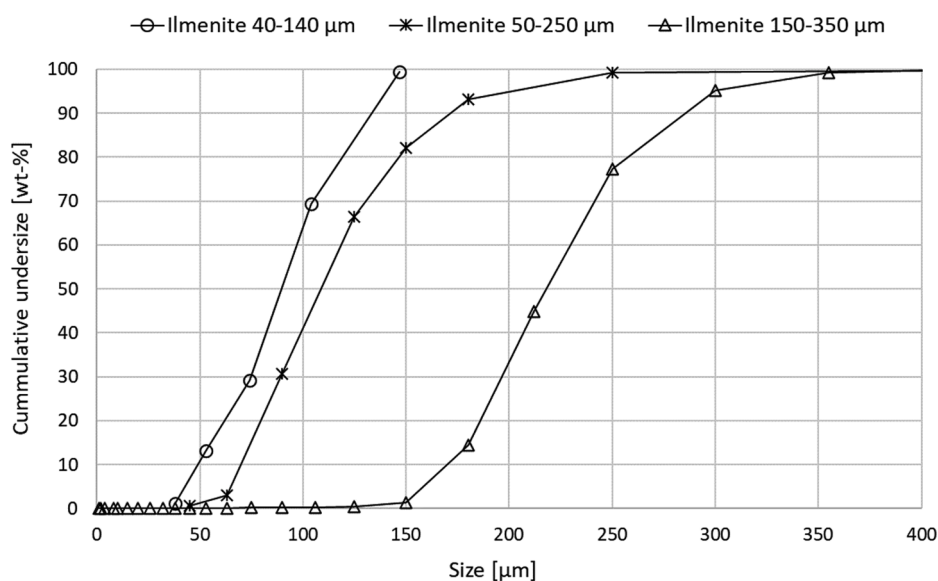
Fig. 7. Particle size distribution of the ilmenite batches used in the tests.

This theoretical riser OC mass flow is not the same as the actual oxygen carrier circulation rate, since only a fraction of the particles flowing upwards in the AR riser follows the gas flow into the cyclone and is transferred to the fuel reactor. As the flow is in the turbulent to fast fluidization regime and not in the transport regime, a large share of the particles falls downwards along the reactor wall, forming an internal recirculation. Studies by Chalmers report that the share of the particles that are transported to the top of the AR that actually leave the reactor through the cyclone was about 29 % in one case and as low as 8 % in another case (Markström and Lyngfelt, 2012; Markström et al., 2014). They point out that this fraction is expected to be different for different reactor designs, superficial velocity, and solids concentration. However, the calculated theoretical AR riser mass flow can be used as a good indication of the relative difference in solid circulation between different operating conditions within the same unit.

The oxygen carrier inventory in the two reactors and lifter is estimated by calculating the average solid-gas mixture density between subsequent pressure transmitters using the pressure difference (Δp) between the transmitters. The densities are multiplied by the volume between the pressure transmitters and summed to give the OC inventory of each reactor and the lifter.

2.5. Uncertainties in results evaluation

2.5.1. Instrument uncertainties

Thermal mass flow controllers (MFC's) are used for feeding inlet gases to the system, except for steam. The MFC's in the system have been checked with a portable flow calibration unit. However, the largest MFC's delivering air to the AR have capacities larger than the calibration unit. This may introduce uncertainties in inlet air flow for the highest flow rates. The MFC's have a given accuracy of ±0.7 % of actual rate.

Gas analysis is done on-line by IR and GC analysers. They are calibrated before and during tests using calibration gases. The gas sampling lines contain heated filters, heated hoses and condensation and filter units. However, very small particles following the FR exhaust stream have on some occasions caused problem by clogging the sampling lines and filters. Improvement to the gas suction lines and additional filtering have reduced this problem. The IR analyser has a given repeatability of ≤ 1 % and the GC has a repeatability of 0.2 – 2.3 %, depending on gas component.

The pressure transmitters (PT's) are used to evaluate inventory and OC balance within the system. They have been checked with a portable

calibration unit. The PT measurement lines were previously flushed manually with a given time interval to prevent plugging from OC particles. The lines could then be partly plugged before it was detected. Later, a continuous flushing system was therefore installed to maintain a small flow that prevent any plugging, causing the PT measurements to operate more accurately. The given accuracy of the PT's is ± 0.065 % of full scale, with full scale being 320 mbar for the PT's used on the pilot unit.

In general, instrument uncertainties are considered being small compared to other uncertainties, as will be presented in the following sub-sections.

2.5.2. Fuel feeding rate and fuel composition

Fuel feeding is done with volumetric screw feeders. The feeding rates of the different fuels are calibrated by running the screw at different rpm's, at room temperature, with the outlet pipe dismantled, allowing feeding into a bucket that is weighed using an accurate scale. Repeated feeding tests of whole pellets in 3 min intervals has shown relative standard deviations of up to 6 %. During operation, the pressure levels upstream and downstream of the fuel screw are balanced with each other, and the pressure downstream is always close to the FR pressure. This should ensure an even feed rate, independent of pressure in the FR. However, it is still some uncertainty in how the feed rate can be affected by the rather large and rapid pressure variations in the FR. Since the screw feeders are calibrated at room temperature, the increase in temperature of the feeding system when operated at normal CLC conditions may also have some effect on the actual fuel feeding rate. The constant flushing of the feeding system with nitrogen helps lower the temperature in the feeding system and hence to minimize this effect. Solid fuels might also be inhomogeneous in nature, however, both the biomass pellets and the petcoke used in the present tests are rather uniform and homogeneous.

2.5.3. Gas flow out of reactors

Since we have good control of the flow of N_2 into both reactors, the N_2 balance can be used to calculate the dry gas flow rates out of the reactors (i.e., the gas flow rate excluding water vapour and condensable components as tars). In our case, the fluidization of the loop seals and lifter is with N_2. A share of this N_2 will flow into the AR and the rest into the FR. It is assumed that half the flow to the AR and FR loop seals, plus 2/3 of the fluidization gas to the lifter, will leave with the gas out from the AR. This may not be fully correct, however, these N_2 flows are very

small compared to the total N_2 from the air inlet to the AR and they will therefore have very limited effect on the calculated balance. Out from the AR it is assumed that it is only CO_2, O_2, and N_2 when measured on dry basis, and since CO_2 and O_2 concentrations are measured, the remaining is N_2. From the N_2 concentration and known N_2 flow through the AR, the total dry gas flow out of the AR is calculated.

The same principle is also used for the FR. The N_2 out from the FR comes from loop-seals and lifter fluidization, and from the fuel feed line. This N_2 amount is known, and the GC measures the N_2 concentration at the FR outlet. From this, the total dry gas flow out of the FR is calculated. The N_2 flow to the FR is much smaller than to the AR and the uncertainty in the distribution of the loop-seals and lifter flows will become more important. In the tests from December 6th 2019 onwards, a more accurate He tracer gas system has been used for the FR. A known quantity of He is fed to the upper part of the FR (to ensure that all is leaving through the FR cyclone), and the GC is measuring the He concentration in the FR exhaust. From this, the total dry gas flow rate out of the FR can be calculated.

2.5.4. Carbon balance

A carbon balance is performed on each test case to check the amount of carbon leaving as carbon-containing gases out of the FR plus carbon leaving the AR as CO_2, in relation to carbon fed with the fuel. The remaining carbon will ideally be the fraction leaving the FR in particulate form, when it is expected that all carbon leaving from AR is in the form of CO_2. This will not give a complete carbon balance since we have no quantitative way to check this amount of carbon-containing particles leaving the FR during a test sequence. Only qualitative information is obtained by SEM (scanning electron microscopy) analysis of the particle (primarily OC) samples taken regularly from the FR exhaust. In addition, the amount of combustible content in the samples from the particle separation bucket, the low-velocity chamber, and the wet scrubber downstream of the FR cyclone can be evaluated using a muffle oven or a carbon analyser. The muffle oven was used on one of the test cases.

2.5.5. Implications of the uncertainties on the main performance parameters

The FR gas conversion efficiency is calculated from the FR exhaust gas analysis and the fuel composition. An error in the gas composition measurement within the specified repeatability of the gas analyzers has small implications on the estimated gas conversion efficiency. To highlight this, we now provide two examples: The calculated gas conversion efficiency for one of the experiments was 76.4%. Increasing the unburnt components CO, CH_4, H_2 and C_2H_4 by 2 %, results in a gas conversion efficiency of 76.0 %. Furthermore, if there is an error in the fuel composition analysis giving 5 % lower stoichiometric oxygen needed per mol carbon (Φ_0), it results in a reduction in the gas conversion efficiency of about 1.2 % points. This implies that the calculated gas conversion efficiencies have reasonably high accuracy.

The CO_2 capture efficiency is calculated from the carbon feed rate (fuel feed rate and carbon content of the fuel) and the carbon flow out of the AR as CO_2. The largest uncertainty here is the solid fuel feed rate. However, if the carbon flow out of the AR is small compared to the carbon fed to the FR, the error in%-points in the CO_2 capture efficiency caused by an error in fuel feed calculation is relatively small. As an example, the CO_2 capture efficiency in the experiment mentioned above was found to be 95 %. If the real fuel feed rate was 6 % lower, the result would be 94.6 %.

The calculation of the OC riser mass flow and OC inventory is dependant on the pressure measurements only. Because of the highly fluctuating pressure in the system, other sources of uncertainty than the accuracy of the pressure transmitters may be important, such as response time and logging frequency. Although these effects will be somewhat smoothed out with time, the riser mass flow and inventory calculations should be considered as approximate values.

2.6. Test procedure

The pilot unit is operated only during daytime, so each test day starts with a heat-up sequence. Fig. 8 shows an overview of the main temperatures and fuel flows for a typical test day. The heat-up sequence starts by heating the air that flows to each reactor by using the 30 kW electric heaters. The pilot burners in each reactor are also ignited, providing about 5 kW each. When the temperatures in the bottom parts of the reactors reach about 350 °C, gaseous fuel injection through the reactor's fuel lances are carefully started, using the pilot burners to ensure that the fuel is ignited and burns. Propane is used in the air reactor and hydrogen in the fuel reactor. Hydrogen is beneficial in the early stage since its high flame speed makes sure the flame is anchored close to the fuel lance holes down in the bed of oxygen carrier, thus efficiently heating the oxygen carrier particles. A hydrogen supply line is currently not installed for the air reactor.

After about five hours the temperatures in the reactor system is above 900 °C, and the temperatures are relatively even throughout the reactor system due to the particle circulation. Then, solid fuel injection into the FR is started while gaseous fuels are turned down and the air to the FR is reduced. If the ilmenite oxygen carrier batch is a fresh one, air to the FR is kept at a small but non-zero value, well below stoichiometric, for a period of more than two hours. This will help activate the ilmenite particles. Some propane is still fired in the AR to support the temperature level. Thereafter, the air to the FR is turned to zero, propane to the AR is shut off, and the unit is in auto-thermal CLC mode. If the ilmenite batch has been used already during previous test campaigns, no activation is required and transfer to full CLC mode is done quickly after the required temperature levels are reached. The propane to the AR can be used also during CLC mode, especially after operational upsets where the system needs to get back to high temperatures as soon as possible. For one of the presented tests, full auto-thermal operation was not achieved, and a small amount of propane to the AR was required to support the temperature level in the AR.

Particle samples can be extracted from the buckets and low-velocity chambers downstream of the exhaust coolers during operation. This will mostly be small fines of oxygen carrier but may also contain some other particulates, such as char and fly ash. Samples from the reactors can only be taken when the unit is stopped and have cooled down. For this reason, the first part of the cool down of the FR is done using nitrogen, to avoid re-oxidation of the particles.

During CLC operation, temperatures, reactor pressures, and inventories are kept as constant as possible, except for small changes made from time to time to try improving the performance. The performance of the pilot unit is evaluated from time-averaging of the measured quantities over time intervals of at least 10 min while the unit is in steady-state operation. This is a fluidized bed system, and even though the operation is stable, some variables, especially the pressures, will fluctuate and the time-averaged values are therefore needed. It is also required that the unit is in stable operation without any changes for at least 10 min prior to the averaging period. The reason that the periods can be this short is the low thermal inertia compared to for example refractory lined units. If temperatures are not changed very much, all reactor quantities adjust rather quickly to new settings, in just some few minutes. For periods with a longer time of stable operation, the averaging period is increased accordingly.

Fig. 9 shows an example where one long and one short period used for time-averaging are indicated. These periods are two of the evaluated test cases shown in Table 2 in the next section. The unstable time between the periods is where the fuel was changed from a mix of milled wood/petcoke to milled wood only. During the second period, with milled wood, the reactor temperatures were slightly and steadily increasing 10 °C during the 11-minutes period. This is not an instability of the system but a response to the heat generation of the system, which is slightly above the cooling effects, providing a steady temperature increase. The AR air pre-heat temperature was reduced 5 °C during this
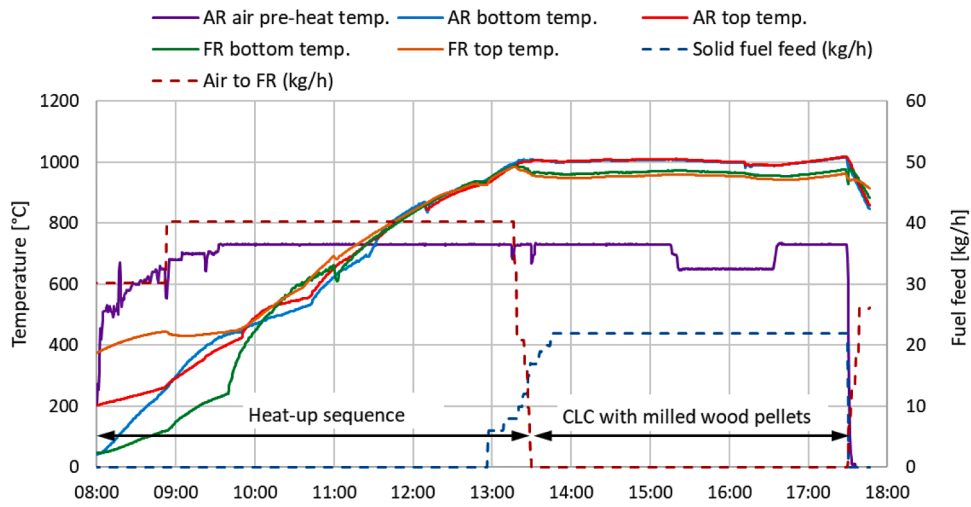
Fig. 8. Overview of typical temperature profiles during a normal one-day test including the heat-up sequence (starting with elevated top temperatures due to 10 kW overnight electric heating).
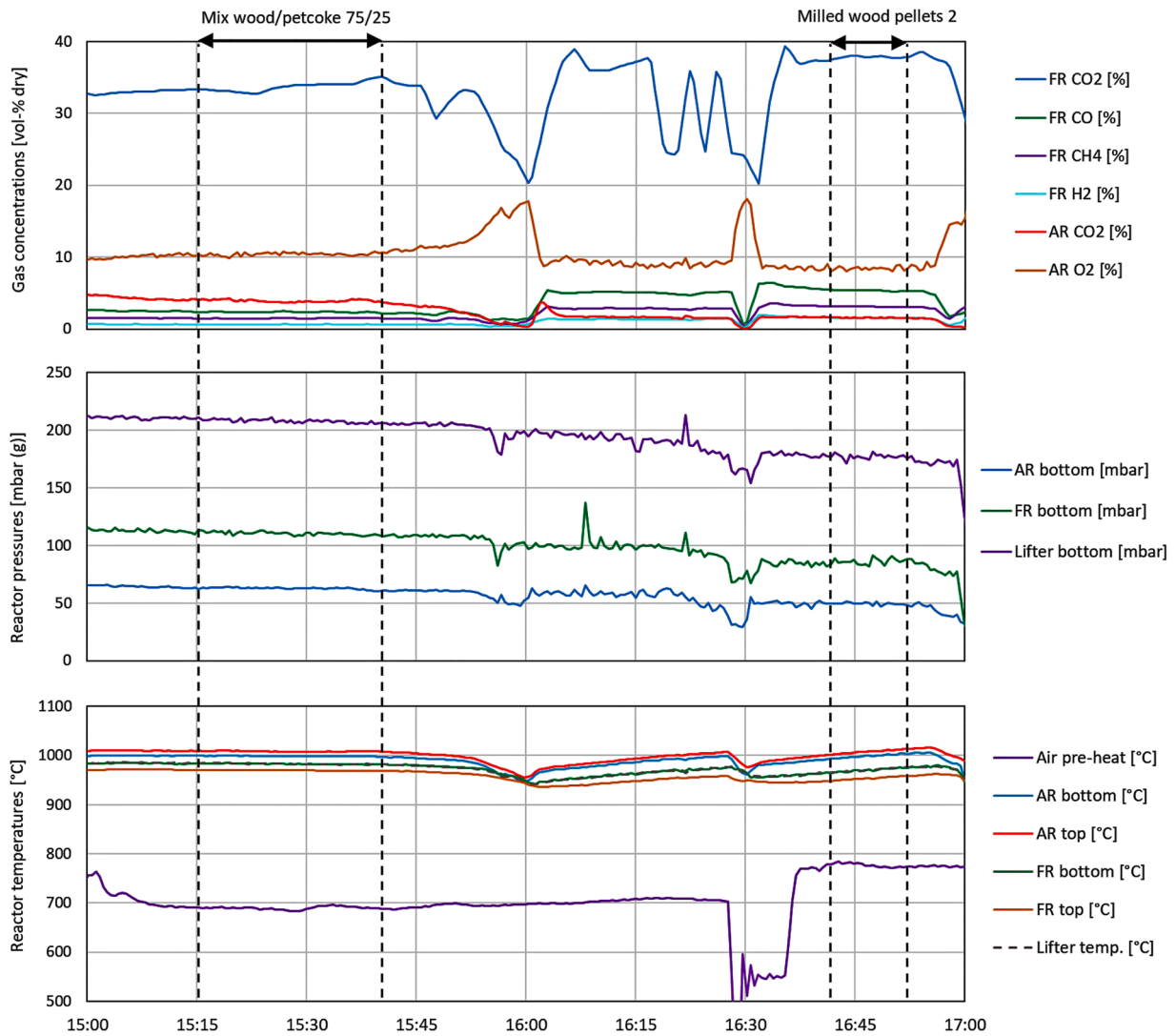

Fig. 9. Example of two periods with stable conditions used for time-averaging. Showing main temperatures, pressures, and gas concentrations.

Table 2

Overview of tests, ilmenite OC size range, fuel type, and test date and period of steady-state conditions used for the time-averaged results evaluation.

Test case	Oxygen carrier size [μm]	Fuel type	Date and averaged time-period
Wood pellets 1	40–140	Wood pellets ø8 mm, batch Arba1	21.09.2018 12:35 – 12:54
Wood pellets 2	50–250	Wood pellets ø8 mm, batch Arba2	15.11.2022 16:30 – 17:29
Milled wood pellets 1	40–140	Milled wood pellets from Arba1, sieved > 800 μm	07.06.2019 14:06 – 14:17
Milled wood pellets 2	40–140	Milled wood pellets from Arba1, sieved > 800 μm	13.06.2019 16:41 - 16:52
Milled wood pellets w/fines 1	40–140	Milled wood pellets from Arba1, un-sieved	06.12.2019 14:07 - 14:31
Milled wood pellets w/fines 2 (*)	150–350	Milled wood pellets from Arba2, un-sieved	04.03.2021 18:40 – 19:15
Mix wood/petcoke 75/25	40–140	Mix of milled and sieved pellets Arba1, and petcoke 315–500 (75/25 wt%)	13.06.2019 15:15 – 15:40
Mix wood/petcoke 50/50	40–140	Mix of milled and sieved pellets Arba1, and petcoke 315–500 (50/50 wt%)	07.06.2019 15:18 – 15:50
Mix wood/petcoke 50/50 w/fines	40–140	Mix of milled and un-sieved pellets Arba1, and petcoke 100–315 w/fines (50/50 wt%)	05.12.2019 20:21 – 20:43
Petcoke 315–500	40–140	Petcoke 315 – 500	07.06.2019 16:34 – 16:48
Petcoke 100–315 w/fines	150–350	Petcoke 100–315 w/fines (40 % < 100 μm)	04.03.2021 20:23 – 21:23

(*) Propane to AR: 11 kW.

time interval but should have been reduced slightly more to get the system fully heat balanced. However, this slight temperature increase does not significantly affect the most important parameters, and the time-averaged values for this period are thus considered relevant for evaluation.

3. Results and discussion

The tests reported in this study were performed over a period of about four years and they are summarized in Table 2. During these four years, improvements to the pilot unit and its operation have been done on the way. All the tests reported here have been performed using ilmenite originating from the Titania mine, in three different size fractions as described in section 2.3. The fuels are based on steam-exploded wood pellets from Arbaflame and a low-sulfur petcoke from China, which have been milled and sieved into different size fractions (cf. section 2.2). The first tests listed in Table 2 are operated with woody biomass only, being the most reactive fuel in this comparison. Fuel sizes range from whole pellets to the smaller milled and sieved pellets, and further to milled and un-sieved pellets, having the smallest average fuel particle size. Next, the reactivity of the fuel is decreased by mixing increasing fractions of petcoke with the wood, until 100 % petcoke is reached.

The operating conditions of the tests are shown in Table 3, where all values are time-averaged over the periods shown in Table 2. The riser mass flow corresponds to the theoretical value calculated according to Eq. (4). The FR inventory is calculated as described in Section 2.4.3 and divided by the solid fuel power to get the specific inventory. The conditions vary quite a bit between the tests, which reflects some of the challenges of controlling a reactor that is autothermal by only a small margin. To maintain the reactor temperatures, and thereby keeping the reactions going, the operating conditions must be tuned for each case. The temperatures, OC circulation rates and inventory distribution cannot be set in the same way as if the reactor had external heating. The reactor temperatures are controlled to a certain extent by adjusting the air inlet temperature. In general, the aim is to be just above 1000 °C in the AR. The temperature in the FR will then stabilize 25 – 50 °C lower than in the AR, depending on particle circulation rate and fuel input. The temperature in the AR is rather even, or increases slightly from bottom to top, while it decreases up along the FR, reflecting the exothermal oxidation reaction in the AR and the close to endothermal reduction

reaction in the FR.

As the gasification rate is strongly temperature dependant, it is advantageous to keep the FR temperature as high as possible. However, the maximum temperature in the reactors should not exceed 1050 °C because of limitations on the structural strength and corrosion resistance of the steel. For the present tests, the temperature in the bottom part of the FR was 956–1021 °C. The highest temperature of 1021 °C was in the special case with the largest size fraction of petcoke as fuel. A large amount of the carbon was lost to the AR where it was immediately burnt, causing very high temperatures both in the AR and the FR. This case is not relevant as a CLC operating condition in an industrial plant.

Table 3 also shows the gas concentrations in the FR and AR exhaust. In the FR, the nitrogen comes from the fluidization of loop seals and lifter, and the nitrogen that is introduced together with the fuel as an aid for the transport into the FR. Nitrogen is also used as fluidization gas in the bottom of the FR in two of the tests ("Wood pellets 2" and "Milled wood pellets 1"), whereas steam is used for the rest of the tests. The FR fluidization gas flow is small compared to the total gas flow in the FR, which mainly consist of volatiles, gasification products, and combustion products from the fuel. Due to the hydrogen content of the wood, a relatively large amount of water is still present in the FR even if nitrogen is used as fluidization gas in the bottom of the FR.

3.1. FR gas conversion and CO_2 capture efficiency

The main performance parameters evaluated in this study are the FR gas conversion efficiency (oxygen demand) and the CO_2 capture efficiency, as described in section 2.4. They are shown in Fig. 10 together with the temperature in the bottom part of the fuel reactor. The presented results are the time-averaged values of the test case periods shown in Table 2. The averaging periods varies between 11 and 60 min but most of them are in the range 20–30 min.

3.1.1. Pure wood cases

The FR gas conversion efficiency for the pure woody biomass cases is around 80 %, which is in accordance with the literature, and in the higher end of what has previously been achieved with biomass and ilmenite (Penthor et al., 2018; Vilches et al., 2017). The highest values of 83 % are obtained for the "Wood pellets 1" and "Milled wood pellets w/fines 2" cases. "Wood pellets 1" has a high specific FR inventory and high FR temperature compared to the other cases. These are two of the

Table 3

Main operating conditions, measured temperatures, and gas concentrations.

Test case	Main operating data				Temperatures					Gas concentrations (on dry gas)							
	Solid fuel power	Air excess λ	Riser mass flow	FR spec. invent.	FR bottom	FR top	AR bottom	AR top	Air pre-heat	FR CO_2	FR CO	FR H_2	FR CH_4	FR C_2H_x	FR N_2	AR CO_2 (*)	AR O_2
	kW_{th}	—	kg/s	kg/MW	°C	°C	°C	°C	°C	vol %	vol %	vol %	vol %	vol%	vol %	vol%	vol %
Wood pellets 1	109	1.5	7.4	253	1006	987	1021	1029	606	47.0	6.3	1.6	2.5	0.1	41.4	1.6	10.1
Wood pellets 2	105	1.3	2.8	190	959	937	1009	1008	675	37.3	7.3	1.9	3.0	0.5	49.8	0.8	10.5
Milled wood pellets 1	101	1.2	3.4	121	986	970	1010	1020	330	39.0	6.2	1.2	2.9	0.2	50.5	1.4	6.5
Milled wood pellets 2	121	1.2	3.8	83	971	954	999	1008	777	38.3	5.4	1.6	3.1	0.4	50.2	1.6	8.4
Milled wood pellets w/ fines 1	120	1.0	3.5	128	964	954	993	1001	860	43.9	6.5	1.8	3.2	0.4	44.0	1.5	6.5
Milled wood pellets w/ fines 2 (*)	129	1.5	8.7	232	956	941	1014	1018	626	49.7	5.7	2.1	2.6	0.5	39.2	0.4	10.7
Mix wood/ petcoke 75/25	79	1.8	4.7	255	983	970	999	1008	690	32.9	2.3	0.6	1.4	0.0	61.6	3.9	10.4
Mix wood/ petcoke 50/50	86	1.6	4.8	263	984	969	1000	1011	777	29.2	1.3	0.4	1.1	0.0	67.9	6.6	9.1
Mix wood/ petcoke 50/50 w/ fines	109	1.0	5.5	262	976	964	1001	1009	860	29.5	2.7	0.8	1.5	0.1	65.4	8.3	4.7
Petcoke 315–500	118	1.2	3.9	200	1021	1004	1025	1051	29	22.4	0.4	0.3	0.4	0.0	76.5	10.4	6.5
Petcoke 100–315 w/fines	116	1.4	9.9	305	975	952	1014	1020	432	17.6	1.7	1.6	1.5	0.0	76.8	8.3	9.5

(*) 11 kW propane to AR is excluded from AR CO_2 concentration.

most important factors affecting FR gas conversion and a high gas conversion should therefore be expected. The "Milled wood pellets w/fines 2" case also has high specific FR inventory. However, the FR temperature is much lower, nearly 50 °C lower than "Wood pellets 1". Still, the FR gas conversion show a high value. One reason can be that 950 °C is a relatively high value compared to many earlier results, and in a temperature range where the effect on the FR gas conversion (oxygen demand) is not that strong as at lower temperatures (Adánez et al., 2018). Another main difference between these two cases is the average fuel particle size. Even though the gasification gases are equally well converted, the capture efficiency of the pellets case is considerably lower with 88 % against 97 %. Since the riser mass flow, and thus the OC circulation rate, is at about the same level for both cases, it cannot explain the difference in carbon capture efficiency. A possible explanation is that the pellets need more time to be gasified due to their larger size, and with the high OC circulation rate the residence time is too short, and a larger share of char is therefore transported to the AR.

Such an effect of fuel size is not that clear when considering the other pellet case "Wood pellets 2". This case has the second highest capture efficiency, which can be explained by the much lower riser mass flow and OC circulation rate. This will leave enough time for the pellets to be gasified while still in the denser part of the OC bed. However, the specific FR inventory and FR temperature are lower in this case compared to "Wood pellets 1", which results in a lower FR gas conversion efficiency.

The two cases "Milled wood pellets 1 and 2" are similar with respect to fuel type, oxygen carrier size, and riser mass flow. "Milled wood pellets 1" has about 15 °C higher FR temperature, and the specific FR inventory is also higher with 120 vs 83 kg/MWh. Therefore, it also

performs slightly better, with 2 %-points higher FR gas conversion efficiency and 1 %-point higher CO_2 capture efficiency. The case "Milled wood pellets w/fines 1" is also rather equal to "Milled wood pellets 1" with respect to oxygen carrier size, specific inventory, and riser mass flow. The main difference is that the average fuel particle size is smaller due to the large share of fines, and the FR average temperature being 19 °C lower. Due to the temperature, it is as expected that the FR gas conversion is slightly lower, but the difference is just less than 1 %-point. The capture efficiency is however slightly higher, 93. % compared to 92.3 % for "Milled wood pellets 1". This may be attributed to the fuel size as discussed above. The milled wood with fines has a large share of smaller particles that have enough residence time to be gasified, whereas the larger sieved milled wood particles are not as much gasified at the same OC circulation rate and OC residence time. A larger share of char is therefore transported to the AR.

The cases "Milled wood pellets w/fines 1 and 2" have the same type of fuel pretreatment and average fuel particle size. The latter case has slightly lower temperature, about 10 °C lower FR average temperature, but a significant higher specific inventory (232 vs 128 kg/MWh). FR gas conversion is thus higher, with 82.8 % vs 79.4 %. The riser mass flow and OC circulation rate is much higher in the "Milled wood pellets w/fines 2" case and this should normally indicate a lower CO_2 capture efficiency. However, this case is the one with the highest capture efficiency of all the presented cases. This case uses pure wood as fuel and the largest OC particles. With these large oxygen carrier particles, it was possible to push the OC circulation to higher level without seeing instabilities in the AR cyclone due to bridging, which can happen with the smaller OC particles when operating at very high temperatures. As long
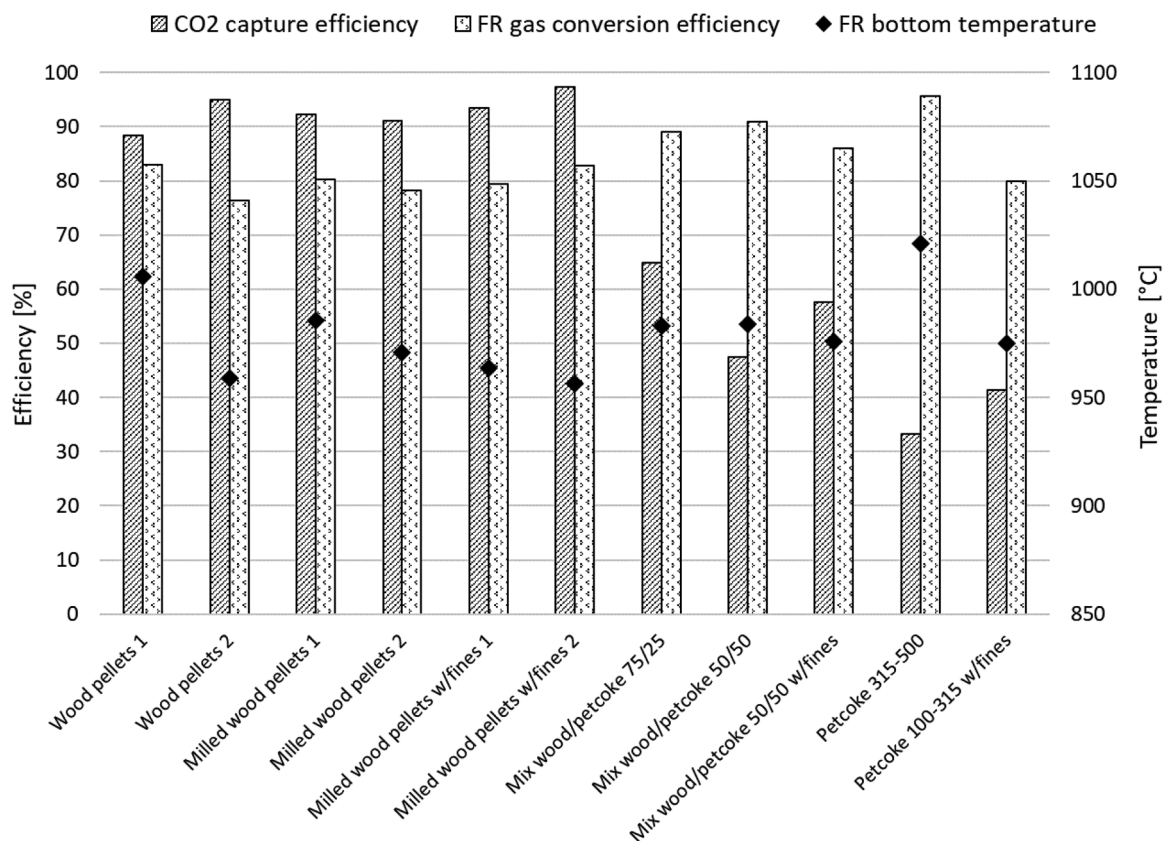
Fig. 10. CO$_2$ capture efficiency, FR gas conversion efficiency, and FR bottom temperature for the 11 evaluated periods.

as the capture efficiency can be maintained, i.e., if the fuel particles are small enough to be gasified even with the higher OC circulation and lower residence time, such a high circulation will be positive in several ways: It will increase the transport of oxygen to the FR, the average oxygen content of the OC in the FR will be higher, providing a higher driving force for oxygen release, and the OC conversion might be lower, meaning the OC will be less reduced in the FR, giving less mechanical stress and possibly increased lifetime. It should be noted that in this case a propane flow equivalent to 11 kW fired heat was supplied to the AR to help keep the temperature at high level. After the test, a damage to the AR insulation that could explain this need for extra heating was discovered. However, the amount of propane was small compared to the air flow and did not affect the OC oxidation, and it is removed from all the calculated parameters, so that the only effect should be to provide high enough temperature of the OC from the AR. Even though the OC out from the AR is at high temperature for this "Milled wood pellets w/ fines 2" case, the temperature in the FR is relatively low. The difference between AR top and FR bottom is 62 °C, whereas for the "Milled wood pellets w/fines 1" it is only 37 °C. This might indicate that there are more OC reduction and fuel conversion reactions happening in the "Milled wood pellets w/fines 2" case, which will need heat from the OC and lower the temperature. This is also in line with the observed higher FR gas conversion and capture rate for this case.

From the above it can be argued that the size of the wood particles matters, however, the trend is not very definite since high CO$_2$ capture efficiency is obtained both for whole pellets and for milled pellets with fines. This may be caused by quick disintegration of the wood pellet when it is introduced to the hot FR bed, leading to less effective difference in particle size. The conversion rate of the char will be independent of size also if the char gasification is kinetically controlled. This means that the internal diffusion of reactant gases inside the char particle is fast compared to the chemical kinetics, which may be the case for relatively small char particles resulting from devolatilization of high volatile fuels

such as woody biomass. The possible quick disintegration of wood pellets means it is converted more or less back to the sawdust it was made from. If solid wood particles, such as wood chips, of same size as the pellets had been used instead, the size of the fuel particles may have had a stronger effect on the conversion process and the capture efficiency.

In any case, most of the present tests with pure woody biomass result in CO$_2$ capture efficiencies well above 90 %, and with FR gas conversion efficiencies of about 80 %. This indicates that for an industrial size CLC reactor system, operating with reactive fuels like woody biomass, a carbon stripper would not be required, since both the CO$_2$ capture efficiency and the gas conversion can be expected to increase due to the much taller reactors and higher residence times at such a scale.

3.1.2. Petcoke cases

The FR gas conversion efficiency is generally higher for the tests with petcoke and mixtures between wood and petcoke. This can be explained by the low amounts of volatiles and gasification products in the FR due to the properties of the petcoke fuel, with very little volatiles and slow char reaction kinetics. A high share of the petcoke is in fact not gasified in the FR but transferred to the AR and combusted there, leading to low CO$_2$ capture efficiencies for these cases. The highest FR gas conversion efficiency is achieved with the largest petcoke particles, and this case also obtains the lowest CO$_2$ capture efficiency (33%). The conversion of the gas in the FR is thus better because of the low amount of gas produced, leading to longer gas residence time. And since most of the fuel is converted in the AR, the OC particles become less reduced in the FR and oxygen for gas conversion is more available.

The effect of the fuel particle size on the CO$_2$ capture efficiency is clearer in the petcoke cases than in the woody biomass cases. This can be seen in the petcoke tests using 50/50 wood/petcoke and pure petcoke (the last four cases in Table 2). The cases involving fines show higher capture efficiency compared to the same fuel without fines, i.e., with larger average fuel particle size. This may be caused by faster

gasification of the small particles, leading to higher gas production and thus less transfer of carbon to the AR. This theory is supported by the FR gas conversion efficiency, which is markedly lower for the cases with the smallest fuel particles, indicating higher production of gas. The effect of the petcoke particle size may also be partially explained by the cyclones not being able to separate out the smallest fuel particles, which means that they will not be transported to the AR with the larger fuel particles.

Gasification of petcoke char at the relevant temperatures is generally slow. Experiments in a lab scale test rig have shown that complete conversion can take up to hours, although this is not directly transferable to a CLC reactor system (Korus et al., 2021). The actual residence time of the fuel particles in the FR is not known, but due to their much lower density than the OC, it is expected to be less than the residence time of the OCs. The OC residence time in the fuel reactor is estimated from OC circulation rate based on the AR riser mass flow and the FR inventory, and it will be less than 1 min in most cases. This means that the fuel particles have residence times that may be significantly shorter than one minute, and for the smallest particles maybe even approaching the gas residence time, which is less than 5 s. Based on this, the total fuel conversion rate in the FR will be low when using petcoke as fuel, even though the FR gas conversion efficiencies show high values. This is also indeed what we find from the experimental tests, where, because of the relatively short particle residence time in the fuel reactor and the lack of a carbon stripper, more than half of the fuel carbon is transferred to the air reactor where it is combusted. This shows that the reactor design of the 150 kW CLC system is not suited for low reactivity fuels because of the short residence time in the FR and the lack of a carbon stripper.

3.2. Carbon balance

Some carbon might leave the fuel reactor in particulate form. The pilot unit does not contain a filter device that can give an accurate measure of such carbon-containing particulates. A full carbon balance is thus not possible to obtain for the present test cases. Instead, the amount of carbon leaving the FR plus AR as gas is calculated from the gas concentrations and the calculated gas flow out of the reactors. This amount of carbon is compared with the amount of carbon fed with the fuel. This "carbon balance" is shown in Fig. 11, where 100 % is equivalent to all carbon fed with the solid fuel is leaving as gas compounds out from FR plus AR. Deviations from 100 % represent carbon leaving the FR as particulates, in addition to measurement uncertainties. It is here anticipated that all carbon particulates transferred to the AR will be rapidly converted to CO_2 and leave as gas. The values above 100 % are unphysical, however, they are within the fuel feed uncertainty as discussed in section 2.5.2.

Ideally, this "carbon balance" says how much carbon is leaving the FR as particulates. The FR gas conversion efficiency is a purely gas-based parameter, giving the oxygen demanded to fully burn-out gaseous components. However, the real oxygen demand in an oxygen-polishing step downstream the FR will also have to burn-out any carbon-containing particulates. For this reason, the carbon balance is performed. Some of the main measurement uncertainties will affect the calculated carbon balance, most notably the uncertainties in fuel feed and gas flow out of reactors described in section 2.5.2 and 2.5.3. This uncertainty in carbon balance will however have no effect on the calculation of FR gas conversion efficiency which is purely based on measured gas concentrations out of the FR, and small effect on the CO_2 capture efficiency as discussed in section 2.5.5.

Four of the test cases are evaluated based on the more accurate He tracer gas for FR flow calculation (cf. section 2.5.3), namely "Wood pellets 2″, "Milled wood pellets w/fines 1 and 2″, and "Petcoke 100–315 w/fines". The two first of these indicates that 4- 5% of the fuel carbon is leaving as particulates or tars. In the latter case, "Petcoke with fines", it seems to be a large loss of carbon particulates out from the FR of more

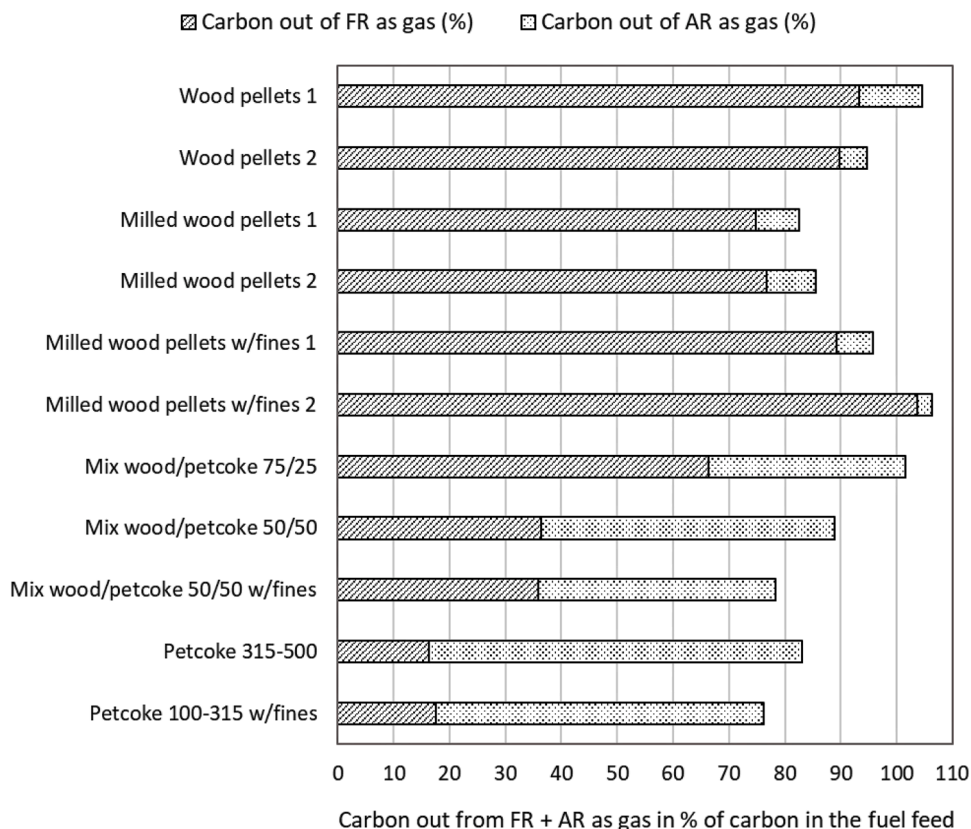**☒ Carbon out of FR as gas (%)**   **☐ Carbon out of AR as gas (%)**

Fig. 11. Carbon out from FR plus AR as gas in percentage of carbon fed to the FR with the solid fuel. Deviation from 100 % is the carbon leaving the FR as particulates plus uncertainties.

than 20 %. Muffle oven evaluation of samples from the FR wet scrubber clearly indicates that there is a particulate loss of carbon, and that these particles are not converted in the simple post-combustion burner primarily meant for gaseous compounds. In the overflow sample from the wet scrubber, the weight loss of the dried sample was as much as 73 %, showing that most of the very small particles following the wet scrubber water overflow are carbon particles. The bottom sample of the wet scrubber showed 26 % weight-loss, meaning less carbon and a higher share of heavier particulates as oxygen carrier fines. These sample evaluations confirm the calculated carbon balance, that in the case with petcoke fuel, there can be a relatively large loss of very small carbon particulates from this pilot unit.

The cases "Wood pellets 1″" and "Milled wood pellets w/fines 2″" have carbon balances of more than 100 %, i.e., the amount of carbon-containing gases from FR + AR is higher than the amount of carbon fed with the solid fuel. The latter case has the highest value, with 106.4 %, of which 103.6 % is carbon out from FR as gas and 2.7 % is carbon out from AR as gas. To give 100 % in sum, the fuel feed rate given by the screw feeder should be 6.5 % higher, or the calculated amount of carbon-containing gas out of FR should be about 6.5 % lower.

The "carbon balance" evaluated above is not a full carbon balance in the sense that not all outlet carbon is measured. Only the gaseous carbon components are measured, and thus, the balance up to 100 % should ideally be carbon particulates following the FR flue gas stream out from the cyclone. Another study (Linderholm et al., 2017) included the mass of particulates leaving with the flue gas, to establish a full mass balance for carbon, nitrogen, and sulfur. The particulates in the flue gas were collected using a wet scrubber and 1 μm filter bags. The results for wood char show that the fulfilment of carbon balance is on average 80 %, with variation from about 65 % to 100 %. This shows that the results in Fig. 11 do not contain larger uncertainty and deviations than other comparable studies.

4. Conclusions

Several CLC tests fuelled by woody biomass, petcoke and mixtures of the two have been conducted in a pilot unit with fuel powers between 79 – 129 kW. The operation is auto-thermal with the preheating of the air to the air reactor as the only external heat source. Three different size fractions of ilmenite have been used as oxygen carriers. Different sizes of the fuel particles have also been tested to see the effect of particle size on the fuel conversion and CO_2 capture efficiency. The CLC unit does not have a carbon stripper, and one of the goals of the study is to conclude whether a carbon stripper can be eliminated when using reactive fuels, such as woody biomass.

CO_2 capture efficiencies up to 97 % was achieved for woody biomass, while for petcoke it was limited to about 40 %. The difference is believed to be caused by the large difference in volatile content and char reactivity between the fuels. The low volatile content and low char reactivity of the petcoke resulted in large amount of char being transferred to the air reactor by the oxygen carrier particle flow. The maximum fuel reactor gas conversion efficiency was 83 % for woody biomass and above 95 % for petcoke. The very high gas conversion efficiency for petcoke is related to the very low capture efficiency. Gasification rates and residence times in the fuel reactor are too low and only a small amount of gas is in fact produced before the char is transported to the air reactor. This low amount of gas is then readily converted.

The fuel particle size has a clear effect on the petcoke and mixtures of petcoke and biomass fuels, with the smallest fuel sizes giving the highest capture efficiencies and lowest fuel reactor gas conversion efficiencies. The size effect is not that clear for the woody biomass fuels, which is believed to be a consequence of the pellets used in our tests, that are steam-exploded pellets made from saw dust. They seem to disintegrate quickly when fed to the fuel reactor, so that the effective fuel size is rapidly reduced. For this reason, solid wood biomass, as wood chips, would most likely show a clearer fuel size effect.

The overall conclusion from the tests is that CO_2 capture efficiencies could be above 95 % in a larger industrial CLC unit operating on biomass, even without a carbon stripper, but that a carbon stripper is needed to reduce the transition of carbon from the fuel reactor to the air reactor for fuels containing less volatiles and with less reactive chars.

Declaration of Competing Interest

The authors declare that they have no known competing financial interests or personal relationships that could have appeared to influence the work reported in this paper.

Data availability

Data will be made available on request.

Acknowledgements

References

IPCC Working Group III report to Sixth Assessment Report, April 2022. Climate Change 2022: mitigation of climate change. (IPCC AR6 WG3). https://www.ipcc.ch/report/ar6/wg3/.

IEA (2021) Net Zero by 2050 - A Roadmap for the Global Energy Sector, IEA, https://www.iea.org/reports/net-zero-by-2050.

IPCC (2018) Global Warming of 1.5°C. An IPCC Special Report on the impacts of global warming of 1.5°C above pre-industrial levels, IPCC, https://www.ipcc.ch/sr15/.

Rydén, M., Lyngfelt, A., Langørgen, Ø., Larring, Y., Brink, A., Teire, S., Havåg, H., Karmhagen, P., 2017. Negative CO_2 emissions with chemical-looping combustion of biomass – a Nordic energy research flagship project. Energy Procedia 114, 6074–6082.

Adánez, J., Abad, A., Mendiara, T., Gayán, P., de Diego, L.F., García-Labiano, F., 2018. Chemical looping combustion of solid fuels. Prog. Energy Combust. Sci. 65, 6–66.

Sun, H., Cheng, M., Chen, D., Xu, l., Li, Z., Cai, N, 2015. Experimental study of a carbon stripper in solid fuel chemical looping combustion. Ind. Eng. Chem. Res. 54, 8743–8753.

Gong, Y., Wang, X., Chen, D., Al-Qadri, B.M.H., 2021. Retrospect and prospect of carbon stripper tehcnology in solid/fuel chemical looping combustion. Fuel Process. Technol. 221.

Spinelli, M., Peltola, P., Bischi, A., Ritvanen, J., Hyppänen, T., Romano, M., 2016. Process integration of chemical looping combustion with oxygen uncoupling in a coal-fired power plant. In: Energy, 103, pp. 646–659.

Lyngfelt, A., Leckner, B., 2015. A 1000 MW_{th} boiler for chemical-looping combustion of solid fuels – Discussion of design and costs. Appl. Energy 157, 475–487.

Fu C., Anantharaman R., Roussanaly S., Yazdanpanah M., Laroche C., Bertholin S. (2021), CLC-CCS plant modelling - Deliverable D5.2 from the CHEERS project, https://cheers-clc.eu/results/.

Roussanaly S., Anantharaman R., Gouraud V., Gaouyat E., Laroche C., Bertholin S. (2022), Studies on CLC-CCS deployment and infrastructure development - Deliverable D5.3 from the CHEERS project, https://cheers-clc.eu/results/.

Lyngfelt, A., Brink, A., Langørgen, Ø., Mattisson, T., Rydén, M., Linderholm, C., 2019. 11,000h of chemical-looping combustion operation—Where are we and where do we want to go? Int. J. Greenhouse Gas Control 88, 38–56.

Yazdanpanah M., Guillou F., Bertholin S., Zhang A. (2018), Demonstration of Chemical Looping Combustion (CLC) with Petcoke Feed for Refining Industry in a 3 MWth Pilot Plant, Proceedings of the 14th International Conference on Greenhouse Gas Control Technologies, Melbourne, Australia, https://doi.org/10.2139/ssrn.3365950.

Grammelis, P., Karampinis, E., Nikolopoulos, A., 2011. Fluidized bed combustion of solid biomass for electricity and/or heat generation. In: Grammelis, P. (Ed.), Solid Biofuels for Energy. Green Energy and Technology. Springer, London. https://doi.org/10.1007/978-1-84996-393-0_6.

Shen, L., Wu, J., Xiao, J., Song, Q., Xiao, R., 2009. Chemical-looping combustion of biomass in a 10 kW_{th} reactor with iron oxide as an oxygen carrier. Energy Fuels 23, 2498–2505.

Mendiara, T., Perez-Astray, A., Izquierdo, M.T., Abad, A., de Diego, L.F., Garcia-Labiano, F., Gayán, P., Adánez, J., 2018. Chemical looping combustion of different types of biomass in a 0.5 kW_{th} unit. Fuel 211, 868–875.

Pérez-Astray, A., Adánez-Rubio, I., Mendiara, T., Izquierdo, M.T., Abad, A., Gayán, P., de Diego, L.F., García-Labiano, F., Adánez, J., 2019. Comparative study of fuel-N and tar evolution in chemical looping combustion of biomass under both iG-CLC and CLOU modes. Fuel 236, 598–607.

Schmitz, M., Linderholm, C., 2018. Chemical looping combustion of biomass in 10-and 100-kW pilots - analysis of conversion and lifetime using a sintered manganese ore. Fuel 231, 73–84.

Ohlemüller, P., Ströhle, J., Epple, B., 2017. Chemical looping combustion of hard coal and torrefied biomass in a 1 MW_{th} pilot plant. Int. J. Greenhouse Gas Control 65, 149–159.

Fleiß, B., Priscak, J., Fuchs, J., Müller, S., Hofbauer, H., 2023. Synthetic oxygen carrier C28 compared to natural ores for chemical looping combustion with solid fuels in 80 kWth pilot plant experiments. Fuel 334. Part 2.

Langørgen Ø., Saanum I. (2018), Chemical Looping Combustion of wood pellets in a 150 kWth CLC reactor. In International Conference on Negative CO2Emissions, May 2018, Gothenburg, Sweden, https://sintef.brage.unit.no/sintef-xmlui/handle/11250/3069380.

Langørgen Ø., Saanum I., Khalil R., Haugen N.E.L. (2022), CLC of waste-derived fuel and biomass in a 150-kW pilot unit, In 6th International Conference on Chemical Looping, 19-22 September 2022, Zaragoza, Spain, https://sintef.brage.unit.no/sintef-xmlui/handle/11250/3084001.

Bischi, A., Langørgen, Ø., Saanum, I., Bakken, J., Seljeskog, M., Bysveen, M., Morin, J.X., Bolland, O, 2011. Design study of a 150kW_{th} double loop circulating fluidized bed reactor system for chemical looping combustion with focus on industrial applicability and pressurization. Int. J. Greenhouse Gas Control 5, 467–474.

Langørgen, Ø., Saanum, I., Haugen, N.E.L., 2017. Chemical looping combustion of methane using a copper-based oxygen carrier in a 150kW reactor system. Energy Procedia 114, 352–360.

Markström, P., Lyngfelt, A., 2012. Designing and operating a cold-flow model of a 100kW chemical-looping combustor. Powder Technol. 222, 182–192.

Markström, P., Linderholm, C., Lyngfelt, A., 2014. Operation of a 100kW chemical-looping combustor with Mexican petroleum coke and Cerrejón coal. Appl. Energy 113, 1830–1835.

Penthor, S., Fuchs, J., Benedikt, F., Schmid, J., Mauerhofer, A., Mayer, K., Hofbauer, H. (2018), First results from an 80kW dual fluidized bed pilot unit for solid fuels at TU Wien, 5th International Conference on Chemical Looping, September 2018, Utah, USA, https://scholar.google.at/citations?view_op=view_citation&hl=de&user=2TeiB68AAAAJ&citation_for_view=2TeiB68AAAAJ:3fE2CSJIrl8C.

Vilches, T.B., Lind, F., Rydén, M., Thunman, H., 2017. Experience of more than 1000h of operation with oxygen carriers and solid biomass at large scale. Appl. Energy 190, 1174–1183.

Korus, A., Klimanek, A., Sładek, S., Szlęk, A., Tilland, A., Bertholin, S., Haugen, N.E., 2021. Kinetic parameters of petroleum coke gasification for modelling chemical-looping combustion systems. Energy 232, 120935.

Linderholm, C., Schmitz, M., Biermann, M., Hanning, M., Lyngfelt, A., 2017. Chemical-looping combustion of solid fuel in a 100kW unit using sintered manganese ore as oxygen carrier. Int. J. Greenhouse Gas Control 65, 170. -18.